Available online at www.sciencedirect.com
SCIENCE DIRECT
Polymer Degradation and Stability 90 (2005) 441–448
Polymer Degradation and Stability
www.elsevier.com/locate/polydegstab

In vitro degradation behaviour of non-porous ultra-fine poly(glycolic acid)/poly(L-lactic acid) fibres and porous ultra-fine poly(glycolic acid) fibres

Young You [a], Sung Won Lee [a], Ji Ho Youk [b], Byung-Moo Min [c], Seung Jin Lee [d], Won Ho Park [a,*]

[a] Department of Textile Engineering, Chungnam National University, 220 Gungdong, Yuseong-ku, Daejeon 305-764, South Korea
[b] Department of Advanced Fibre Engineering, Division of Nano-Systems, Inha University, Incheon 402-751, South Korea
[c] Department of Oral Biochemistry, College of Dentistry, Seoul National University, Seoul 110-749, South Korea
[d] College of Pharmacy, Ewha Wowans University, Seoul 120-750, South Korea

Received 17 February 2005; received in revised form 6 April 2005; accepted 12 April 2005
Available online 14 June 2005

Abstract

The in vitro degradation behaviour of non-porous ultra-fine poly(glycolic acid)/poly(L-lactic acid) (PGA/PLA) fibres and porous ultra-fine PGA fibres was investigated. The non-porous ultra-fine PGA/PLA fibres were prepared by electrospinning of a PGA/PLA solution in 1,1,1,3,3,3-hexafluoro-2-propanol and the porous ultra-fine PGA fibres were obtained from them via selective removal of PLA with chloroform. Since PLA has a lower degradation rate than PGA, the degradation rates of the ultra-fine PGA/PLA fibres decreased with increasing content of PLA. The porous ultra-fine PGA fibres were degraded in vitro in the order of non-porous PGA > P-PGA/PLA(90/10) > P-PGA/PLA(70/30) > P-PGA/PLA(50/50) > P-PGA/PLA(30/70) due to autocatalytic hydrolysis.

Keywords: Poly(glycolic acid); Poly(L-lactic acid); Electrospinning; Porous ultra-fine fibre; Biodegradability

1. Introduction

Electrospinning is a unique technique for preparation of non-woven mats of ultra-fine fibres, exhibiting high specific surface area and high porosity [1]. Interestingly, it is possible to electrospin porous ultra-fine fibres by using highly volatile solvents [2]. A porous structure can be generated by phase separation resulting from the evaporation of solvents during the electrospinning process. The polymer-rich phase forms the fibre matrix and the solvent-rich phase the pores. However, the rapid evaporation of solvents induces the blockage of a spinning tip and prevents continuous electrospinning. Porous ultra-fine fibres can also be prepared via the electrospinning of immiscible polymer pairs, followed by removal of one component from the phase-separated composite fibres via selective dissolution, thermal degradation or photo degradation [3–7]. It was suggested that these porous ultra-fine fibres have potential applications in nanofiltration and functional nanotubes [8–10].

Poly(glycolic acid) (PGA), poly(L-lactic acid) (PLA), and poly(lactic-*co*-glycolic acid) (PLGA) have been widely used in biomedical fields because they have good biodegradability, biocompatibility, and mechanical properties [11–13]. Recently, the electrospinning of these polymers has attracted a great deal of attention

* Corresponding author. Tel.: +82 42 821 6613; fax: +82 42 823 3736.
E-mail address: parkwh@cnu.ac.kr (W.H. Park).

0141-3910/$ - see front matter © 2005 Elsevier Ltd. All rights reserved.
doi:10.1016/j.polymdegradstab.2005.04.015

due to their potential applications in drug delivery, surgical implantation, enzyme immobilization, tissue regeneration, prevention of post-operative induced adhesion, etc. [14–21]. In our previous study [7], porous ultra-fine PGA fibres were prepared via a selective dissolution technique. Ultra-fine PGA/PLA fibres were first prepared by electrospinning a PGA/PLA solution in 1,1,1,3,3,3-hexafluoro-2-propanol (HFIP) and then most of PLA was removed with chloroform. PGA and PLA were immiscible and that a co-continuous phase morphology was developed during the electrospinning process.

In this study, in vitro degradation behaviour of the non-porous ultra-fine PGA/PLA fibres and the resulting porous ultra-fine PGA fibres were investigated. It was reported that ultra-fine PGA, PLA, and PLGA fibres were degraded in the order of PGA > PLGA ≫ PLA [22]. The average diameters of the ultra-fine PGA, PLA, and PLGA fibres were 310, 290, and 760 nm, respectively. For biomedical applications, a suitable degradation rate is one of the most important requirements for matrix materials. It is expected that porous ultra-fine PGA fibres will show different biodegradability according to their porosity.

2. Experimental

2.1. Materials

PGA (M_w = 14,000–20,000) and PLA (M_w = 450,000) were purchased from Purac Co. and Boehringer Ingelheim, respectively. HFIP and chloroform were purchased from Aldrich Co. and used as received.

2.2. Electrospinning of PGA/PLA blend solutions

In order to prepare PGA/PLA blend solutions, 8 wt% of PGA and 5 wt% of PLA solutions in HFIP were prepared and mixed at predetermined ratios (PGA/PLA = 90/10, 70/30, 50/50, 30/70 w/w). The electrospinning setup used in this study consisted of a syringe and needle (ID = 0.495 mm), an aluminium collecting plate, and a high voltage supply (Chungpa EMT). All the PGA/PLA solutions were electrospun at a positive voltage of 17 kV and a working distance of 7 cm (the distance between the needle tip and the collecting plate). The mass flow rate of the PGA/PLA solutions was 4 mL/h.

2.3. Preparation of porous ultra-fine PGA fibres

Porous ultra-fine PGA fibres were prepared from non-porous ultra-fine PGA/PLA fibres via selective dissolution of PLA with chloroform. The porous ultra-fine PGA fibres obtained from the non-porous ultra-fine PGA/PLA fibres are referred to as P-PGA/PLA fibres. For example, porous ultra-fine PGA fibres obtained from ultra-fine PGA/PLA(90/10) fibres are referred to as P-PGA/PLA(90/10) fibres.

2.4. In vitro degradation

Ultra-fine fibre mats were cut into a rectangular shape with dimensions of 40 × 40 × 0.1 mm, placed in closed bottles containing 50 mL of phosphate buffer solution (PBS, pH 7.3), and then incubated in vitro at 37 °C for different periods of time. After each degradation period, the samples were washed, dried in a vacuum oven at 25 °C for 24 h, and then weighed. The weight-loss percentages of the samples were calculated from the dried weights obtained before and after degradation.

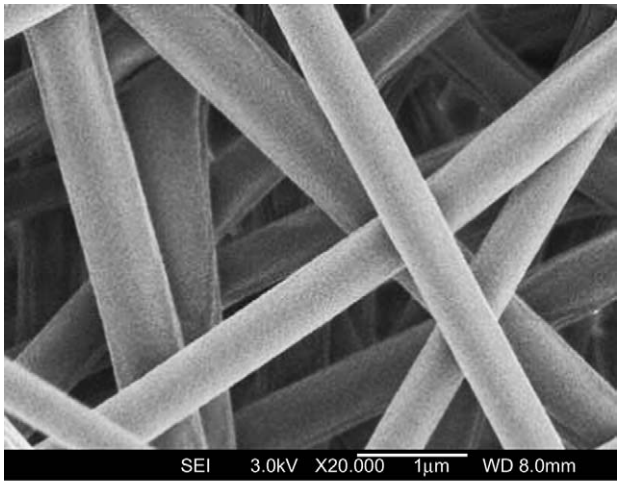

(a)

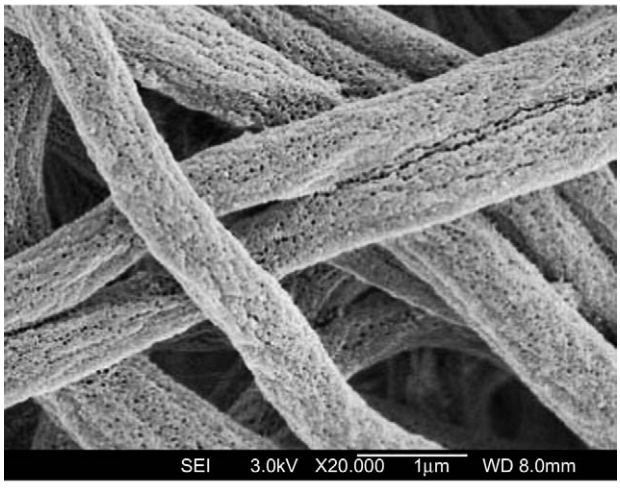

(b)

Fig. 1. SEM images of (a) ultra-fine PGA/PLA(50/50) fibres and (b) P-PGA/PLA(50/50) fibres.

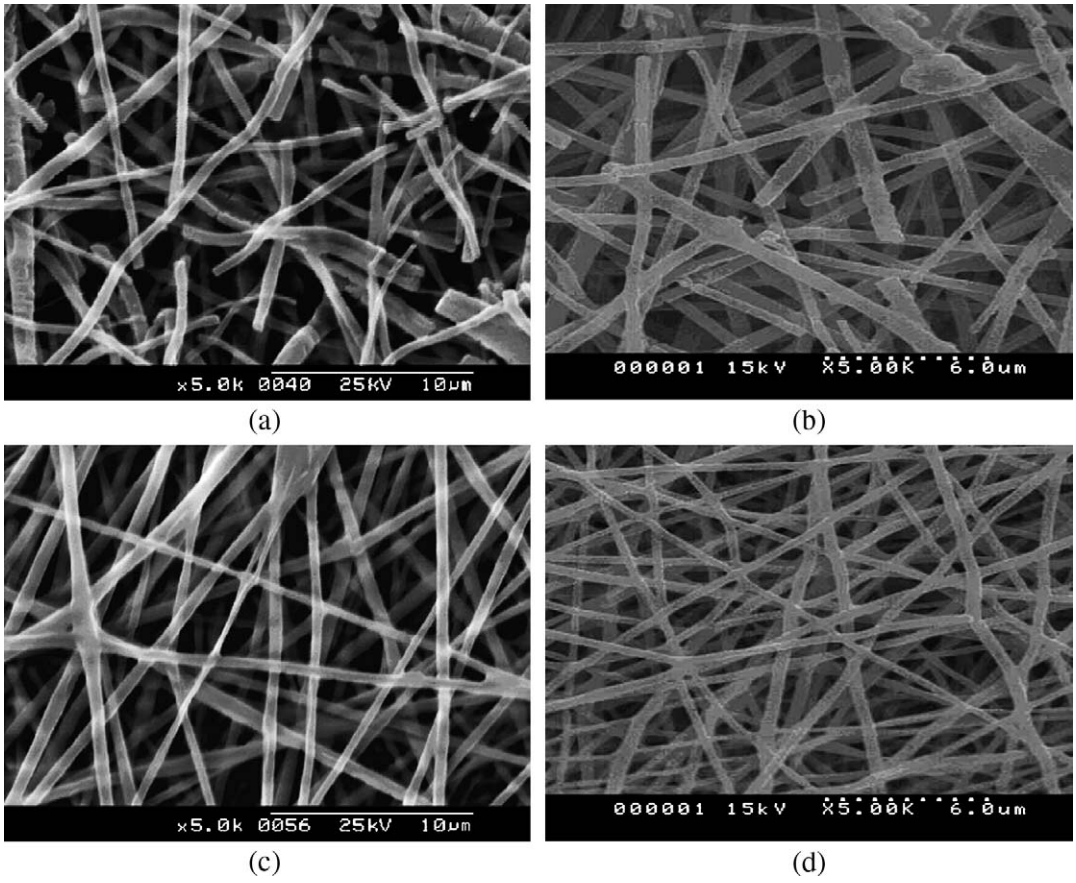

Fig. 2. Morphological changes in ultra-fine PGA/PLA fibres after 8 days of in vitro degradation: (a) PGA/PLA(90/10), (b) PGA/PLA(70/30), (c) PGA/PLA(50/50), and (d) PGA/PLA(30/70).

2.5. Characterization

The morphology of ultra-fine fibres was observed by a field emission scanning electron microscope (FE-SEM, JSM-6335F, JEOL). Prior to the observation, platinum was coated by ion sputtering for a few seconds. Differential scanning calorimetry (DSC) measurements were conducted with a Perkin–Elmer DSC-7 under a nitrogen atmosphere. About 10 mg of sample was sealed in an aluminium pan for the measurements. In order to remove thermal history, the sample was heated to 250 °C, held at this temperature for 1 min, and then quenched to 10 °C. The sample was reheated to 250 °C at a heating rate of 20 °C/min. The crystalline type in ultra-fine fibres was analysed on a wide angle X-ray diffractometer (model D/max-IIB, Rigaku International Corp.).

3. Results and discussion

3.1. Porous ultra-fine PGA fibres

Fig. 1 shows the representative SEM images of non-porous ultra-fine PGA/PLA fibres and porous ultra-fine PGA fibres obtained therefrom (for more details see Ref. [7]). In this study, non-porous ultra-fine PGA/PLA(90/10), PGA/PLA(70/30), PGA/PLA(50/50), and PGA/PLA(30/70) fibres were electrospun. The average diameters of the ultra-fine PGA/PLA fibres ranged from 200 to 500 nm. Porous ultra-fine PGA fibres were prepared from the ultra-fine PGA/PLA fibres via selective dissolution of PLA with chloroform. After the PLA extraction, the resulting PGA fibres were round-shaped and had three-dimensionally interconnected pores with a circular shape. With increasing the content of PLA in the ultra-fine PGA/PLA fibres, the resulting ultra-fine PGA fibres had a thinner wall thickness between pores.

3.2. In vitro degradation of non-porous ultra-fine PGA/PLA fibres

Fig. 2 shows the morphological changes in the non-porous ultra-fine PGA/PLA fibres after 8 days of in vitro degradation. Ultra-fine PGA/PLA(90/10) and PGA/PLA(70/30) fibres were broken down into short fibre fragments. However, no significant morphological change was observed for ultra-fine PGA/PLA(50/50)

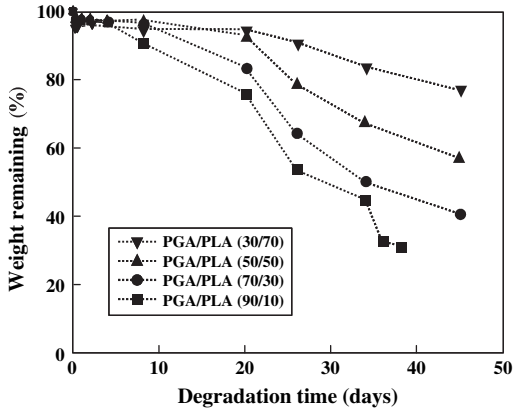

Fig. 3. The weight loss of ultra-fine PGA/PLA fibres according to the degradation time.

and PGA/PLA(30/70) fibres. Fig. 3 shows the weight loss of the ultra-fine PGA/PLA fibres according to the degradation time. It is known that PLA has a lower degradation rate than PGA due to its hydrophobic methyl group in the repeating unit. Also, in this study, the molecular weight of PGA was much lower than that of PLA. As expected, the degradation rates of blend fibres decreased with increasing content of PLA. The residual weight of the PGA/PLA(90/10) fibres was about 40% after 35 days, while that of the PGA/PLA(30/70) was over 80%. Fig. 4 shows the changes in thermal properties of the ultra-fine PGA/PLA fibres during in vitro degradation. PGA usually has higher crystallinity than PLA. It was found in our previous study that crystallinities of ultra-fine PGA and PLA fibres were first increased by the cleavage-induced crystallization and then gradually decreased during in vitro degradation [22]. The melting endotherm of PGA (~220 °C) in the ultra-fine PGA/PLA fibres became weaker and broader after 8 days as the degradation of crystalline regions in PGA started. In the case of PGA/PLA(50/50) fibres, the melting endotherm of PGA almost disappeared after 26 days. In contrast, the melting endotherm of PLA (~180 °C) became stronger and slightly shifted to lower temperatures as PGA was degraded preferentially. Fig. 5 shows the WAXD patterns of the ultra-fine PGA/PLA fibres during in vitro degradation. For ultra-fine PGA/PLA(90/10) and PGA/PLA(70/30) fibres, the characteristic WAXD

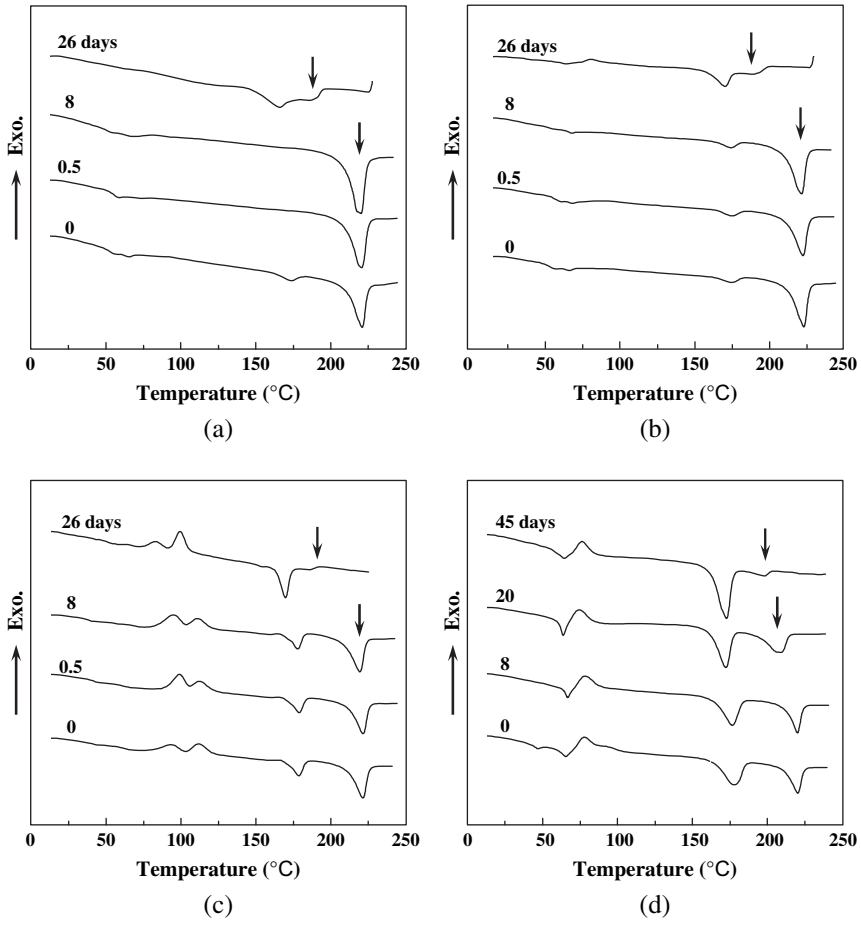

Fig. 4. DSC thermograms for ultra-fine PGA/PLA fibres during in vitro degradation: (a) PGA/PLA(90/10), (b) PGA/PLA(70/30), (c) PGA/PLA(50/50), and (d) PGA/PLA(30/70).

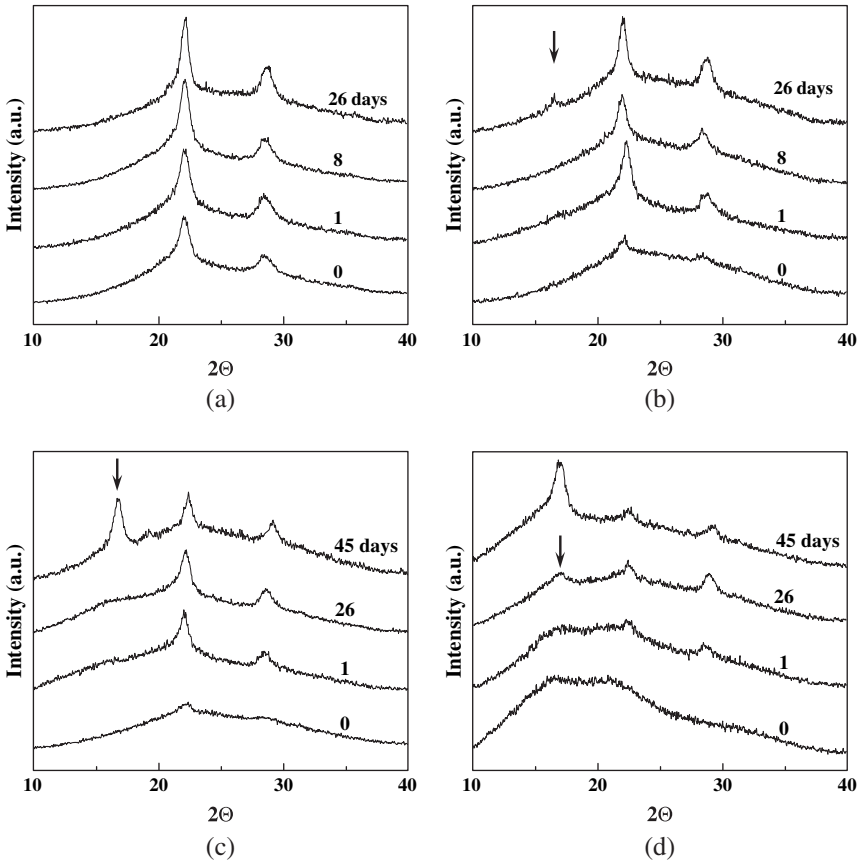

Fig. 5. WAXD patterns of ultra-fine PGA/PLA fibres during in vitro degradation: (a) PGA/PLA(90/10), (b) PGA/PLA(70/30), (c) PGA/PLA(50/50), and (d) PGA/PLA(30/70).

peaks for PGA at 22° and 29° were clearly observed, which were assigned to (110) and (020) planes, respectively [23]. In cases of ultra-fine PGA/PLA(50/50) and PGA/PLA(30/70) fibres, the diffraction peak at ~16° corresponding to the most distinctive peak for crystalline PLA appeared and became stronger according to the degradation time due to the crystallization of PLA.

3.3. In vitro degradation of porous ultra-fine PGA fibres

Fig. 6 shows the morphological changes in the porous ultra-fine PGA fibres after 8 days of in vitro degradation. P-PGA/PLA(90/10), P-PGA/PLA(70/30), and P-PGA/PLA(50/50) fibres showed very similar morphological changes to their original ultra-fine PGA/PLA fibres after 8 days of in vitro degradation. However, P-PGA/PLA(30/70) fibres showed a porous membrane-like structure (Fig. 6(d)). As observed in our previous study, the P-PGA/PLA(30/70) fibres had a somewhat flat shape after extraction of PLA. This highly porous three-dimensionally interconnected fibre structure was collapsed and adhered together during in vitro degradation. Fig. 7 shows the weight loss of the porous ultra-fine PGA fibres according to the degradation time. Their degradation rates were lower than that of non-porous ultra-fine PGA fibres, which were electrospun from an 8 wt% PGA solution in HFIP and had average diameter of 301 nm. Interestingly, porous ultra-fine PGA fibres resulted from a lower PLA content showed a higher degradation rate. The degradation rates of aliphatic polyesters were affected by numerous parameters such as molecular characteristics, crystallinity, and crystalline thickness. It was reported that the degradation rate of PLGA films was increased with increasing thickness from 10 to 100 μm [24], which resulted from a greater extent of the autocatalytic hydrolysis [24–27]. The degradation proceeded more rapidly in the centre of the thicker film due to the autocatalytic action of carboxylic acid end groups and degradation products that were trapped in the matrix. It is considered that the degradation rate of the porous ultra-fine PGA fibres is affected by the autocatalytic hydrolysis. With increasing the content of PLA in ultra-fine PGA/PLA fibres, the resulting ultra-fine PGA fibres had a thinner wall thickness between pores. Consequently, the P-PGA/PLA(30/70) fibres were degraded most slowly due to the fastest diffusion of the degraded products.

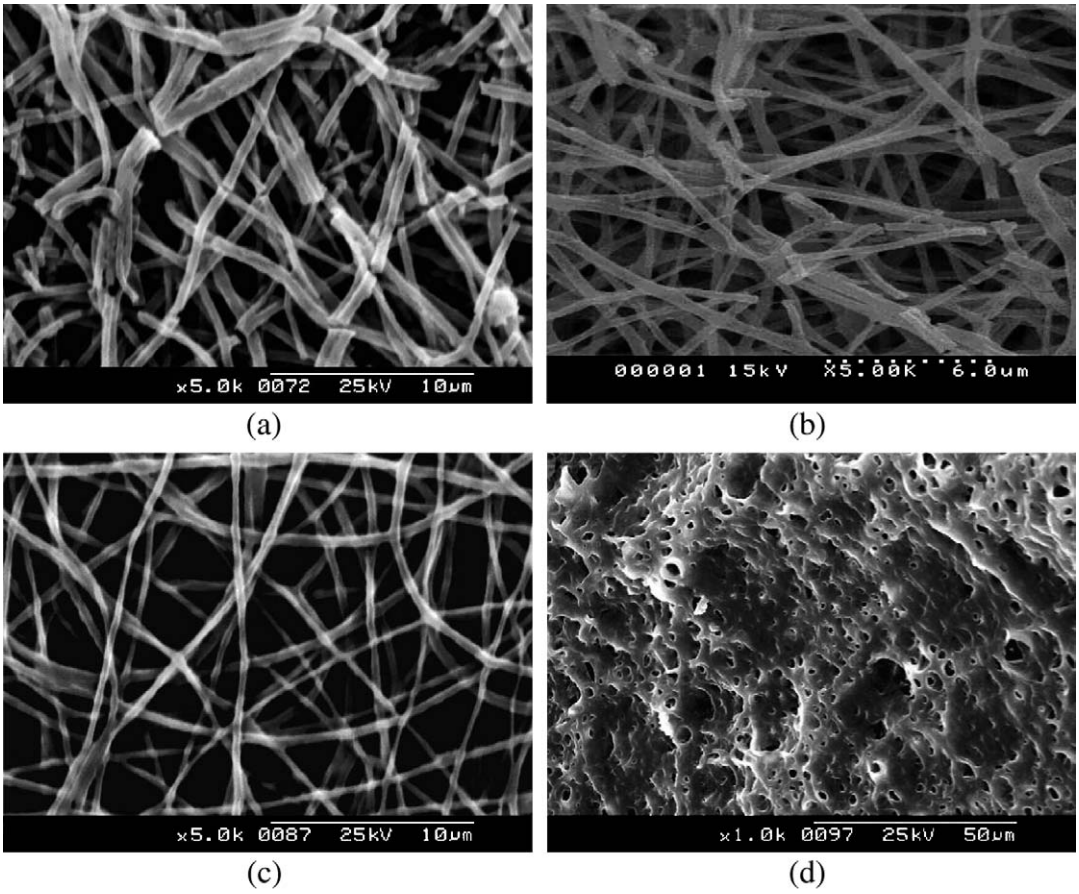

Fig. 6. Morphological changes in porous ultra-fine PGA fibres after 8 days of in vitro degradation: (a) P-PGA/PLA(90/10), (b) P-PGA/PLA(70/30), (c) P-PGA/PLA(50/50), and (d) P-PGA/PLA(30/70).

Figs. 8 and 9 show the changes in DSC thermograms and WAXD patterns of the porous ultra-fine PGA fibres during in vitro degradation, respectively. In the case of P-PGA/PLA(90/10) fibres, the melting endotherm of PGA became weaker and broader after 8 days. The two characteristic WAXD peaks for PGA at 22° and 29° became stronger in the early stage and weaker after 8 days of in vitro degradation. These results are in good accordance with our previous study that the crystallinity of ultra-fine PGA fibres was increased for 2 days by the cleavage-induced crystallization and then gradually decreased during in vitro degradation. The tie molecules in amorphous regions degraded and that the crystallization in the amorphous regions became more effective. For P-PGA/PLA(70/30), P-PGA/PLA(50/50), and P-PGA/PLA(30/70) fibres, the reflection peak at ~16° was observed due to the crystallization of residual PLA.

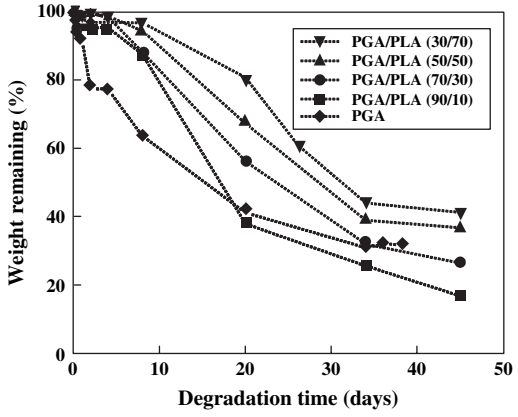

Fig. 7. The weight loss of porous ultra-fine PGA fibres according to the degradation time.

4. Conclusions

The non-porous ultra-fine PGA/PLA fibres were degraded in vitro in the order of PGA/PLA(90/10) > PGA/PLA(70/30) > PGA/PLA(50/50) > PGA/PLA(30/70). In the case of the porous ultra-fine PGA fibres, they were degraded in the order of non-porous PGA > P-PGA/PLA(90/10) > P-PGA/PLA(70/30) > P-PGA/PLA(50/50) > P-PGA/PLA(30/70) due to the autocatalytic hydrolysis. The crystallinities of the non-porous ultra-fine PGA/PLA and the porous PGA fibres were first increased by the cleavage-induced crystallization and then gradually decreased during in vitro degradation.

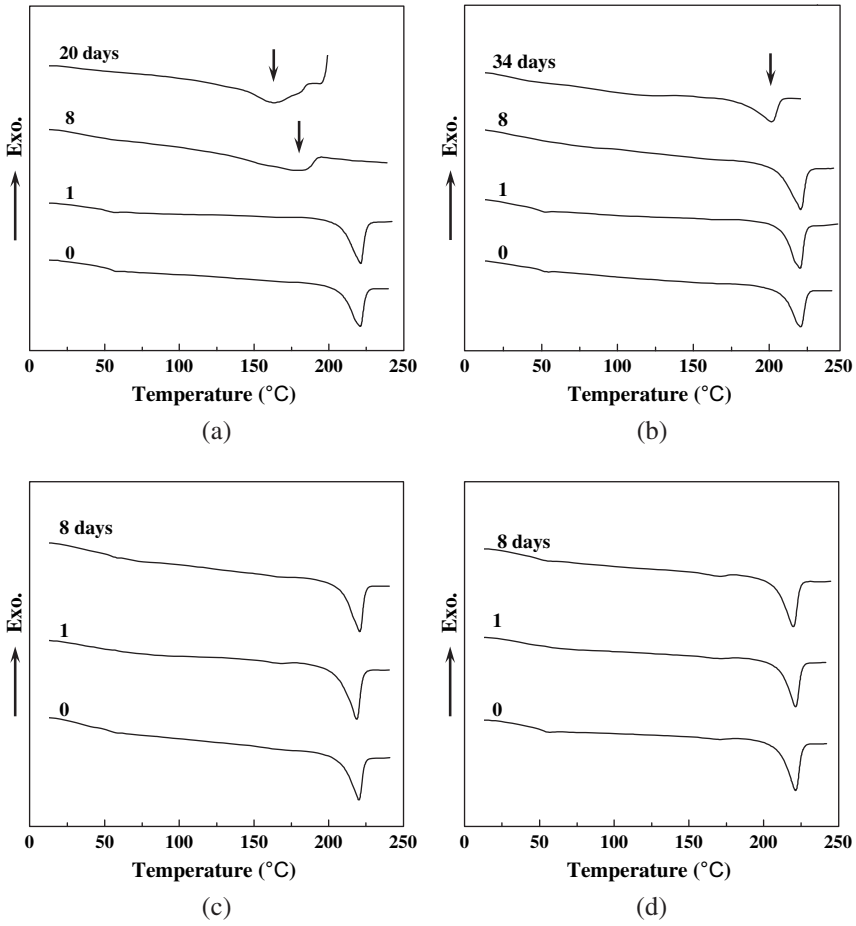

Fig. 8. DSC thermograms of porous ultra-fine PGA fibres during in vitro degradation: (a) P-PGA/PLA(90/10), (b) P-PGA/PLA(70/30), (c) P-PGA/PLA(50/50), and (d) P-PGA/PLA(30/70).

Acknowledgments

This work was supported by the Ministry of Science and Technology, Korea.

References

[1] Huang ZM, Zhang YZ, Kotaki M, Ramakrishna S. A review on polymer nanofibres by electrospinning and their applications in nanocomposites. Compos Sci Technol 2003;63:2223–53.
[2] Bognitzki M, Czado W, Frese T, Schaper A, Hellwig M, Steinhart M, et al. Nanostructured fibres via electrospinning. Adv Mater 2001;13:70–2.
[3] He CH, Gong J. The preparation of PVA–Pt/TiO_2 composite nanofibre aggregate and the photocatalytic degradation of solid-phase polyvinyl alcohol. Polym Degrad Stab 2003;81:117–24.
[4] Li D, Xia Y. Fabrication of titania nanofibres by electrospinning. Nano Lett 2003;3:555–60.
[5] Li D, Wang Y, Xia Y. Electrospinning of polymeric and ceramic nanofibres as uniaxially aligned arrays. Nano Lett 2003;3:1167–71.
[6] Han SO, Son WK, Cho D, Youk JH, Park WH. Preparation of porous ultra-fine fibres via selective thermal degradation of electrospun polyetherimide/poly(3-hydroxybutyrate-*co*-3-hydroxyvalerate) fibres. Polym Degrad Stab 2004;86:257–62.
[7] You Y, Youk JH, Lee TS, Min BM, Lee SJ, Park WH. Preparation of porous ultra-fine PGA fibres via selective dissolution of electrospun PGA/PLA blend fibres. Mater Lett, submitted for publication.
[8] Bognitzki M, Hou H, Ishaque M, Frese T, Hellwig M, Schwarte C, et al. Polymer, metal, and hybrid nano- and mesotubes by coating degradable polymer template fibres. Adv Mater 2000;12:637–40.
[9] Caruso RA, Schattka JH, Greiner A. Titanium dioxide tubes from sol-gel coating of electrospun polymer fibres. Adv Mater 2001;13:1577–9.
[10] Hou H, Jun Z, Reuning A, Schaper A, Wendorff JH, Greiner A. Poly(*p*-xylylene) nanotubes by coating and removal of ultrathin polymer template fibres. Macromolecules 2002;35:2429–31.
[11] Wu XS. Synthesis and properties of biodegradable lactic/glycolic acid polymers. In: Encyclopedic handbook of biomaterials and bioengineering. New York: Marcel Dekker; 1995. p. 1015–54.
[12] Wu XS. Preparation, characterization, and drug delivery applications of microspheres based on biodegradable lactic/glycolic acid polymers. In: Encyclopedic handbook of biomaterials and bioengineering. New York: Marcel Dekker; 1995. p. 1151–200.
[13] Anderson JM, Shive MS. Biodegradation and biocompatibility of PLA and PLGA microspheres. Adv Drug Deliver Rev 1997;28:5–24.
[14] Kenawy ER, Bowlin GL, Mansfield K, Layman J, Simpson DG, Sanders EH, et al. Release of tetracycline hydrochloride from electrospun poly(ethylene-*co*-vinylacetate), poly(lactic acid), and a blend. J Control Release 2002;81:57–64.

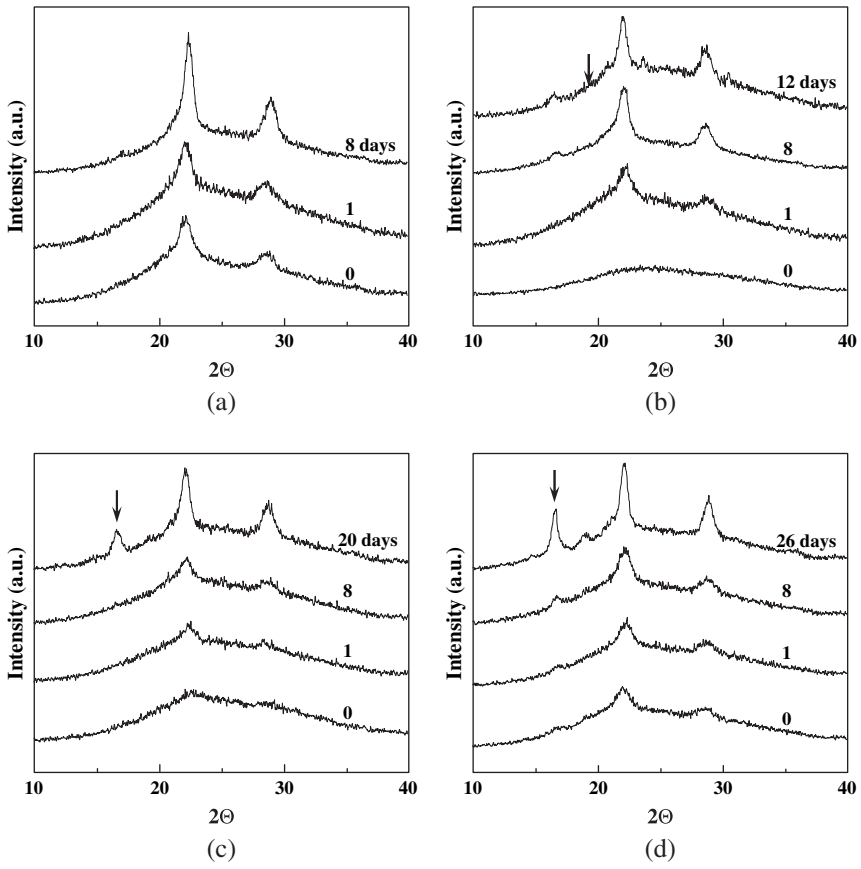

Fig. 9. WAXD patterns of porous ultra-fine PGA fibres during in vitro degradation: (a) P-PGA/PLA(90/10), (b) P-PGA/PLA(70/30), (c) P-PGA/PLA(50/50), and (d) P-PGA/PLA(30/70).

[15] Zong X, Kim K, Fang D, Ran S, Hsiao BS, Chu B. Structure and process relationship of electrospun bioabsorbable nanofibre membranes. Polymer 2002;43:4403–12.
[16] Zong X, Ran S, Kim KS, Fang D, Hsiao BS, Chu B. Structure and morphology changes during in vitro degradation of electrospun poly(glycolide-*co*-lactide) nanofibre membrane. Biomacromolecules 2003;4:416–23.
[17] Luu YK, Kim K, Hsiao BS, Chu B, Hadjiargyrou M. Development of nanostructured DNA delivery scaffold via electrospinning of PLGA and PLA-PEG block copolymers. J Control Release 2003;89:341–53.
[18] Zeng J, Xu X, Chen X, Liang Q, Bian X, Yang L, et al. Biodegradable electrospun fibres for drug delivery. J Control Release 2003;92:227–31.
[19] Zong X, Ran S, Fang D, Hsiao BS, Chu B. Control of structure, morphology and property in electrospun poly(glycolide-*co*-lactide) non-woven membranes via post-draw treatments. Polymer 2003;44:4959–67.
[20] Zeng J, Chen X, Liang Q, Xu X, Jing X. Enzymatic degradation of poly(L-lactide) and poly(ε-caprolactone) electrospun fibres. Macromol Biosci 2004;4:1118–25.
[21] Kim K, Luu YK, Chang C, Fang D, Hsiao BS, Chu B, et al. Incorporation and controlled release of a hydrophilic antibiotic using poly(glycolide-*co*-lactide)-based electrospun nanofibrous scaffolds. J Control Release 2004;98:47–56.
[22] You Y, Min BM, Lee SJ, Lee TS, Park WH. In vitro degradation behavior of electrospun polyglycolide, polylactide, and poly(lactide-*co*-glycolide). J Appl Polym Sci 2005;95:193–200.
[23] Wang ZG, Wang X, Hsiao BS, Andjelic S, Jamiolkowski D, McDivitt J, et al. Time-resolved isothermal crystallization of absorbable PGA-*co*-PLA copolymer by synchrotron small-angle X-ray scattering and wide-angle X-ray diffraction. Polymer 2001; 42:8965–73.
[24] Lu L, Garcia CV, Mikos AG. In vitro degradation of thin poly(DL-lactide-*co*-glycolic acid) films. J Biomed Mater Res 1999; 46:236–44.
[25] Lee JW, Gardella JA. In vitro hydrolytic surface degradation of poly(glycolic acid): role of the surface segregated amorphous region in the induction period of bulk erosion. Macromolecules 2001;34:3928–37.
[26] Tsuji H. Autocatalytic hydrolysis of amorphous-made polylactides: effects of L-lactide content, tacticity, and enantiomeric polymer blending. Polymer 2002;43:1789–96.
[27] Tsuji H. In vitro hydrolysis of blends from enantiomeric poly(lactide)s. Part 4: well-homo-crystallized blend and non-blended films. Biomaterials 2003;24:537–47.